Anal Bioanal Chem (2006) 384: 667–682
DOI 10.1007/s00216-005-0236-x

REVIEW

Ralf Lucklum · Peter Hauptmann

Acoustic microsensors—the challenge behind microgravimetry

Received: 24 August 2005 / Revised: 16 November 2005 / Accepted: 17 November 2005 / Published online: 30 December 2005

Abstract Acoustic microsensors are commonly known as high-resolution mass-sensitive devices. This is a restricted view in many chemical and biosensor applications, especially in liquids. Sensitivity to non-gravimetric effects is a challenging feature of acoustic sensors. In this review we give an overview of recent developments in resonant sensors including micromachined devices and also list recent activity relating to the (bio)chemical interface of acoustic sensors. Major results from theoretical analysis of quartz crystal resonators, descriptive for all acoustic microsensors are summarized and non-gravimetric contributions to the sensor signal from viscoelasticity and interfacial effects are discussed. We finally conclude with some future perspectives.

Keywords Resonant microsensors · Acoustic sensors · Cantilever sensors

Introduction

Acoustic microsensors are a versatile class of physical, chemical, and biological sensors known to be cost-effective, high-resolution, mass sensing devices. Their history began in 1959 when Sauerbrey published the essential relationship between the change of the resonant frequency of a quartz crystal and the mass added to its surface [1]. He consequently named the sensor the quartz crystal microbalance (QCM). Its use to monitor film thickness (growth) has been standard measurement technology for many decades in vacuum-deposition units. Other physical sensor applications with market relevance are temperature and pressure sensors, reviewed elsewhere [2]. The first application of quartz crystals as chemical sensors was reported by King [3]. The QCM has evolved to enable measurement in applications in analytical chemistry, electrochemistry, and biochemistry, because of its sensitivity at the transducer surface–analyte interface. It can detect monolayers of small molecules, complex arrays of biopolymers and biomacromolecules, or whole cells.

The name microbalance implies that acoustic sensors measure mass or mass changes only. Indeed, in many applications acoustic sensors are used to convert a mass accumulated on the surface into a frequency shift. In chemical and, especially, biochemical applications, however, this basic understanding of the sensor principle can easily lead to misinterpretation of experimental results, especially when working in a liquid environment. It also hinders recognition by the experimenter of the outstanding capabilities of quartz crystal resonator sensors and other acoustic devices not available to other sensor principles. In a more general view acoustic sensors enable sensitive probing of changes within films attached to the transducer surface and at solid–solid and solid–liquid interfaces and are not restricted to mass changes [4]. Effects other than mass changes, so called non-gravimetric effects, can, moreover, be expected to contribute significantly to sensor response [5, 6]. Energy dissipation phenomena at its interface, a feature principally different from the mass effect, are just one obvious aspect.

Systematic application of non-gravimetric effects is a challenging task and requires a theoretical background both in chemistry or biochemistry, to enable prediction or estimation of specific property changes in the materials involved in the detection process, and in acoustics, to enable understanding of the path of signal transduction and estimation of changes in the (electrical) sensor signal. Manufacturing knowledge, including preparation technology, to optimize the signal-generation and transduction process of interest and to minimize the effect of unavoidable experimental variations, is also required.

In the text below we give a short review of recent developments of acoustic-wave-based sensors and the challenges behind microgravimetry. We start with a short overview of traditional and new acoustic sensors. It is not our intention to discuss chemical or biochemical aspects of acoustic sensors—we merely provide a list of very recent publications reporting improved chemical or biological sensitivity (for early papers, see references therein). The theoretical background of the sensor principle, based on

R. Lucklum (✉) · P. Hauptmann
Institute for Micro and Sensor Systems (IMOS),
Otto-von-Guericke-University, Magdeburg,
P.O. Box 4120, 39016 Magdeburg, Germany
e-mail: Ralf.Lucklum@et.uni-magdeburg.de

acoustic wave propagation, will be summarized, but only as much as is necessary to enable understanding of the challenges of acoustic wave-based sensors behind microgravimetry. We also concentrate on quartz crystal resonators, because the results are representative for acoustic sensors. Finally we draw some perspectives of acoustic sensors.

Acoustic microsensors

The output signal of acoustic microsensors usually used is a frequency. Frequency is an analog value but can easily be converted into a digital signal, e.g. by counting the number of cycles in a defined period of time. In typical electrical circuitry the acoustic sensor is the frequency-determining element of an oscillator. Analysis of several solutions, ranging from oscillators to impedance analyzers, is given elsewhere, e.g. [7, 8]. Conversion of the mechanical resonant frequency into the electrical oscillation frequency does not cause loss of resolution. Transmission reliability of a frequency signal is very secure. Together with the high working frequency of acoustic devices it enables preparation of wireless sensors [9–11]. Frequency is insensitive to variations in the signal amplitude, drift, and bias. The vibration amplitude carries independent information and is therefore also used in modern acoustic sensor concepts. Because these advantages are common to all resonant sensors, it is not surprising that resonant sensors have attracted increasing interest in recent years.

Several acoustic devices have also been used as microsensors: surface acoustic wave (SAW) devices, surface transverse wave (STW) devices, flexural plate wave (FPW) devices, Love wave (LW) devices, and shear horizontal acoustic plate mode (SH-APM) devices are well known. For overviews of working principles, application features including (mass) sensitivity see, e.g., Refs. [12–15] and for graphic sketches, see, e.g. Ref. [16]. Some more specific devices not yet widely used are fiber acoustic wave (FAW) devices [17], tube acoustic wave devices [18, 19], and, most recently, a ball SAW device [20]. The concept of FAW devices is similar to FPW devices. A fiber can be as thin as a few micrometers, leading to very high sensitivity. Tube acoustic devices are very attractive from a packaging point of view, because the tube can act as liquid container; a measurement cell is not required. The sensitivity varies inversely with wall thickness. The advantage of ball SAW devices is a reduction of insertion losses, because of strong reduction of aperture. Film bulk acoustic resonator (FBAR) devices [21, 22] and micromechanical resonant structures, up to now mostly cantilevers, are the MEMS-based variant [23, 24]. Similar to the history of traditional acoustic sensors, improvements of the transducer element have been driven by different requirements, e.g. frequency normal [25–27] (quartz crystals), filter [28–31] (SAW, FBAR devices), and atomic-force microscopy [32–35] (cantilever).

Improvement of sensitivity is still a driving force in sensor development. Sticking again with the mass sensitivity argument, mass sensitivity of resonant sensors is basically governed by the ratio of mass change to the overall vibrating mass. As an approximation, the lighter the resonator the larger the relative mass increase, because of a bound mass. FPW devices have been a successful attempt to optimize mass sensitivity. In contrast to SAW devices (in which the vibrating mass is defined by the penetration depth of the acoustic wave and decreases with frequency) FPW devices can also be applied in liquids. Another attempt is quartz crystals with largely increased fundamental frequencies [36, 37]. These resonators have also been fabricated as arrays (Fig. 1) [38–40].

Another important development applies a technique known from non-destructive testing for acoustic wave generation. The so-called magnetic-acoustic-resonator sensor (MARS) uses a planar coil to generate an electromagnetic field at radio frequency [41, 42]. This field induces eddy currents in a metallic film deposited on the surface of a non-piezoelectric resonator. Lorentz forces appear in a strong static magnetic field and drive the resonator. They are capable of exciting several acoustic waves, including the shear mode, if the frequency of the applied current coincides with the respective resonant frequency of the resonator. Figure 2 shows the model used for FEM simulation. The key issue of this concept is a high quality factor (Q) of the mechanical resonator. Therefore several materials have been tested. A Q-factor above 10^5 has recently been achieved with micromachined silicon membranes [43]. In a slightly different version the same principle has been applied to electrodeless quartz crystals [44, 45]. In this composition a D-field similar to that in the traditional configuration with electrodes arises, because of the specific properties of the permittivity tensor of AT-cut quartz [46]. One important advantageous feature of this concept is the capability of exciting harmonics up to the GHz range [47–49].

Micromachined devices

Silicon technology can lead to new possibilities—the capability to detect even smaller mass, the capability to

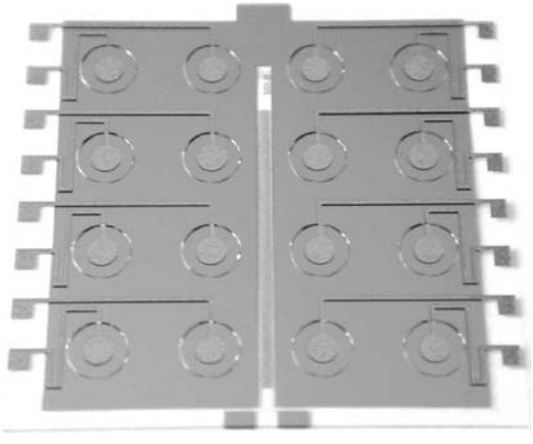

Fig. 1 4x4 quartz crystal sensor array. The membrane of each sensor element has been thinned by wet etching. The resonance frequency of each sensor could be elevated to frequencies up to 50 MHz [40]

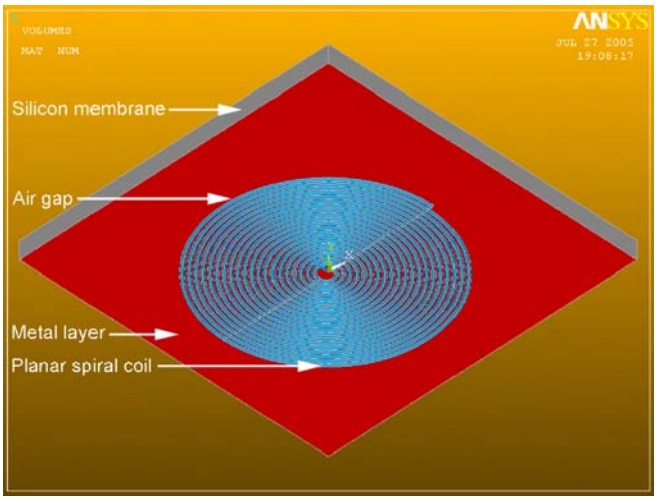

Fig. 2 Basic model for FEM simulation. Eddy currents are caused by an RF current through the planar coil. Lorentz forces in the metal layer appear in a superposed static magnetic field, which is generated from a permanent magnet (not shown) [43]

fabricate arrays with a much larger number of elements per unit area, the capability of monolithically integrated electronic circuitry, and mass production at low cost. The available technology can also be adapted for sensor surface modification with specific coatings to create chemical selectivity. Nowadays commercial cantilevers are usually used. They are typically made of silicon, silicon nitride, or silicon dioxide. A great variety of dimensions and shapes is available. As sensors cantilevers can be used in the resonant or non-resonant mode. In the resonant mode mass deposited on to the cantilever reduces its resonant frequency. Assuming constant properties of the cantilever, frequency shift is proportional to mass change. The cantilever acts similar to the QCM. The proportional factor, and hence the mass sensitivity, depends on the force constant, which is a function of geometry and the apparent Young's modulus. In reality length and width can be well controlled during the etching process. The thickness of the beam is not usually known precisely enough. Although the Young's modulus of the cantilever also deviates from bulk values, accurate methods enable exact calibration of the sensor.

One example of a non-resonant application is the stress generated bending. Changes in surface stress can be the result of physical interaction, for example electrostatic forces between charged molecules on the surface, or of chemical nature, e.g. analyte absorption-induced swelling of a chemically sensitive coating during chemical sensing, conformational changes in a polymer film because of thermal treatment or radiation induced cross-linking, changes in surface energy, etc. In typical sensor arrangements this stress is not compensated at the opposite side of the cantilever and results in bending of the cantilever. This non-resonant application demonstrates the high sensitivity of those devices to factors other than mass. A review of cantilever applications in both principles of operation, including theoretical background, deflection detection techniques, and actuation methods is given elsewhere [50–52]; for very recent new activities see Refs. [53–62].

In liquid applications the resonant principle seems to be the more robust method whereas bending gives access to new fascinating applications based on structural changes in thin adsorbed layers. The resonant mode needs active driving of the cantilever and feedback for frequency measurement. Piezoelectric materials, for example PZT, are often used for that purpose; magnetic actuation [63] or pulsed laser heating [64] have also been applied. Cantilevered AT-cut quartz-crystal resonators have been fabricated by deep reactive ion etching [65]. One major challenging issue is an improved quality factor of the resonator. Q-factors of approximately 10^3 in the upper kHz frequency range in air enable a mass resolution in the picogram range. Magnetic actuation and a closed feedback loop can enhance the quality factor substantially [66]. A parametric resonance amplification has shown to provide a 1–2 orders of magnitude increased sensitivity compared with the simple harmonic resonance mode in air [67]. Another method for improved mass sensitivity is the use of higher modes. Because of the appearance of nodes additionally to the points of clamping, the resonant frequency change also depends on the position the mass is applied [68].

In a liquid environment, especially in biosensing applications, the out-of-plane vibration of the cantilever is strongly damped and results in an essentially reduced Q-factor of a few tens only. It can be enhanced by incorporating the cantilever in an amplifying feedback loop. With a monolithically integrated differential feedback circuit and a cantilever with electromagnetic actuation and piezoresistive readout a frequency stability of 3 Hz at a resonant frequency of about 200 kHz in water could be achieved [69]. Another approach avoids the out-of-plane vibration. A disc-shaped microstructure operates in a rotational in-plane mode with resonance frequencies between 300 and 700 kHz, Fig. 3. The open-loop Q-factor has been found to be as high as 5800 in air and 100 in water [70]. A very different approach avoids viscous damping by feeding the analyte through channels buried in the cantilever, Fig. 4 [71]. The cantilever still vibrates in air; the mass change occurs within the channels because of adsorption of the molecules of interest on the channel

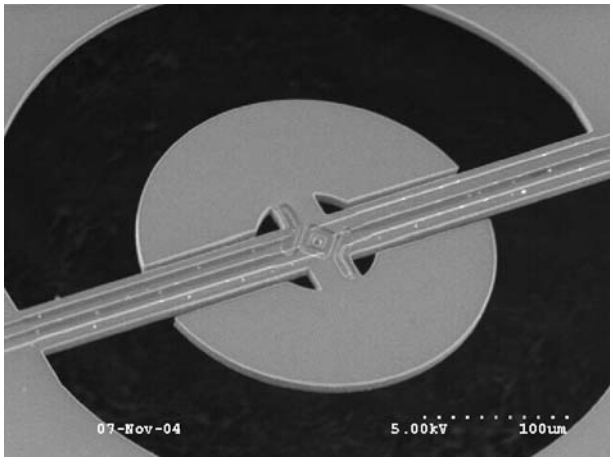

Fig. 3 SEM photograph of a high Q disk-shaped micromachined resonator [70] (reproduced with kind permission of J.H. Seo)

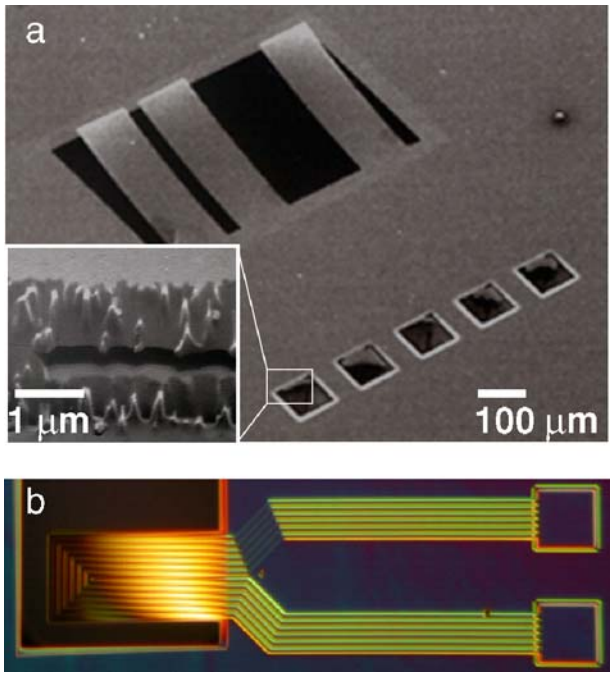

Fig. 4 SEM micrographs of cantilever with buried microchannels [71] (reproduced with kind permission of S. Manalis)

walls. The sensor signal is actually based on density differences between the attached molecule and the buffer.

FBAR devices use a piezoelectric thin film for acoustic wave generation. They can have resonant frequencies in the GHz range. To keep this advantage the piezoelectric film is deposited on a micromachined silicon membrane. Another approach traps acoustic energy within a thin layer of a bulky silicon substrate, using several different layers with very different acoustic impedances, which act as acoustic mirror. This solution is especially interesting for sensing applications, because it solves the problem of fragility. The capability of this class of devices for chemical sensing has been reported elsewhere, e.g. Ref. [72]; for recent device developments and applications see Refs. [73–77].

Another group of acoustic sensors—ultrasonic sensors—should be mentioned here. This group of sensors shares some features with acoustic microsensors but there are also some remarkable differences. Similar to acoustic microsensors the acoustic wave is usually generated and detected with a piezoelectric device. In contrast, the acoustic wave travels through the bulk of the material of interest. Similarly, acoustic wave then carries information of both geometric and material properties of all materials along the acoustic path. Distance (level) or flow sensors and non-destructive testing are just two well known examples of a variety of applications of ultrasonic sensors.

Ultrasonic sensors have also proven their capabilities as chemical sensors, especially in process monitoring. These use the dependence of sound velocity, attenuation, and, nowadays, acoustic impedance on material properties relevant to process control, especially of complex liquid mixtures [78, 79]. Recently a MEMS version of ultrasonic sensors has been introduced, so-called capacitive micromachined ultrasonic transducers (cMUT) [80–82] and, recently, Refs. [83–86]. Instead of capacitive driven, piezoelectric excitation of vibration of a membrane at radio frequency is also possible [87]. Those transducers close the gap between acoustic microsensors and ultrasonic sensors and are very promising for microfluidic applications [88].

Chemical interface

Acoustic sensors are uniquely sensitive to the mass of molecular species. This is a unique advantage but also requires precautions to avoid any unwanted interaction with other species. Cross sensitivity is therefore a major issue of the microbalance principle, whether with quartz crystals or other acoustic devices.

Acoustic sensors are inherently non-specific. The core of chemical analysis involving surfaces is a method for immobilization of the target molecule on the surface of the transducer. This issue is being addressed in various ways. King's approach to achieve chemical sensitivity and selectivity by modifying the surface of the quartz crystal with a chemically sensitive film is still standard technology. He started with materials used in gas chromatography as stationary phase. Meanwhile an extremely large variety of materials has been used for that purpose: numerous polymers [89–95], organometallic compounds [96–98], dendrimers [99–102], synthetic molecular recognition materials, including supramolecular substances [103], and molecular imprinted polymers [104–113] biomaterials [114–120] including DNA [121–128], proteins [129–140], cells [141] nanomaterials [142–146] and others.

The separation between transformation of a (bio)chemical signal into a physical signal in the film or on its surface and transformation of the physical signal into an electrical signal in the acoustic device is an advantage acoustic sensors share with other sensor principles. It enables use of the transducer device in many very different applications. The specification is mainly a question of selection or development of the appropriate sensitive material and the appropriate preparation technology and hence mainly a question of surface chemistry and application to complex (bio)molecular systems.

Other issues must be addressed to enable commercial competition with the success of other methods, especially surface plasmon resonance (SPR) instruments. A major challenge is a reproducible coating procedure without the need for expensive sensor calibration, irrespective of whether a self assembled monolayer, immobilization of a biomolecule, or a thick polymer film. It includes minimization of unspecific binding or any other loading of the sensor surface. The acoustic device must also be re-usable. Although inexpensive in principle, application of acoustic sensor in liquids, especially, requires devices with enhanced properties. Examples of cost-intensive special features of quartz-crystal sensors are a well polished smooth surface to prevent liquid trapping, specific electrode geometry to achieve a large grounded electrode, to prevent crosstalk to

the electrical properties of a contacting liquid, e.g. a buffer solution, and a contact stripe which goes round the edge to provide electrical contacts on one side of the crystal; gold as electrode material both to furnish a noble surface and also as the basis for stable and reliable surface functionalization is also required. Mechanical stability of the electrode is another major concern in terms of re-usability. The availability of commercially pre-activated acoustic sensors would greatly reduce the requirement for skilled operators, simplify measurement procedures and reduce the overall measurement time. As far as we are aware quartz crystals modified for specific applications are available from Q-Sense only [147].

Theoretical considerations

The theoretical background of electroacoustic devices is well developed. Several models are available, very basic physical models and equivalent circuit models [148–159]. In terms of description of sensor behavior they deliver very similar results. Acoustic microsensors are characterized by different prevailing acoustic modes. Quartz crystal resonators work with a thickness-shear wave, SAW sensors exploit a Rayleigh wave; both waves are transverse whereas the typical bending mode of cantilevers generates a longitudinal wave. It has, however, been shown that under typical experimental conditions acoustic microsensors transform the acoustic properties of the coating(s) and, if so, of a liquid, into equivalent electrical signals. When modeling wave propagation, one usually decomposes the wave vector into lateral components and a component normal to the main surface of the device. Important features common to all devices result from the vertical component. It obeys laws similar to those valid for quartz crystal resonators—hence the challenges behind the physics are also similar. The results derived for quartz crystal resonators cover the most important findings and are representative for acoustic microsensors. They are summarized below.

1. The basic principle of operation of a generic acoustic-wave sensor is a traveling wave in a confined structure which produces a set of standing waves whose frequency is determined jointly by the velocity of the traveling wave and the dimensions of the confining structure. The most basic method of resonator modeling consequently requires application of the theory of wave propagation taking into consideration the properties of the material and the geometric dimensions of the resonator.
2. A quartz crystal resonator (QCR) as used for chemical or biochemical sensing is a resonator composed of the piezoelectric crystal itself and at least one (non-piezoelectric) layer to achieve chemical sensitivity. In the transmission line model (TLM), one of the most successful tools for sensor analysis, a composite resonator, is represented as an arrangement of the respective number of transmission lines in series. Each transmission line has two acoustic ports and represents one layer. The large aspect ratio between the lateral dimensions and the thickness of each layer enables one-dimensional treatment of wave propagation. The inherent assumption is that the material is homogeneous within one layer. The TLM also requires continuity of particle displacement and shear stress at the interface between all transmission line elements.
3. Acoustic properties of coating(s) and liquid are summarized in one value which is recognized by the piezoelectric transducer: the (effective surface) acoustic load (impedance), Z_L e.g. Ref. [160]. The acoustic load plays the central role for any chemical acoustic microsensor. It does not play any role if the acoustic load is generated by a simple mass (per area), as introduced by Sauerbrey, by a semi-infinite liquid, as first analyzed by Kanazawa, because of the viscoelastic properties of a single layer or from a multilayer arrangement. The acoustic load carries all acoustically relevant information, which is related to the chemical or biochemical interaction irrespective of whether a change in Z_L is generated by pure mass accumulation or if the interaction is accompanied by a change in material properties. Interfacial property changes between layers have also been found to produce significant changes of Z_L.
4. The TLM can be represented in an equivalent circuit consisting of two impedances in series parallel to C_0, Fig. 5. C_0 is the only electrical element; the two impedances represent acoustic properties of the sensor. This branch is, therefore, called the motional arm. Z_{mq} represents the acoustic properties of the quartz crystal only. As is common for sensors, Z_{mq} is assumed to be constant. Z_{mL} is the electrical representation of the acoustic load, Z_L.
5. The plot of the electrical admittance vs. frequency of the circuitry (see, e.g., Ref. [161]) has several characteristic points which can be used for measurement, e.g. maximum or minimum of the admittance

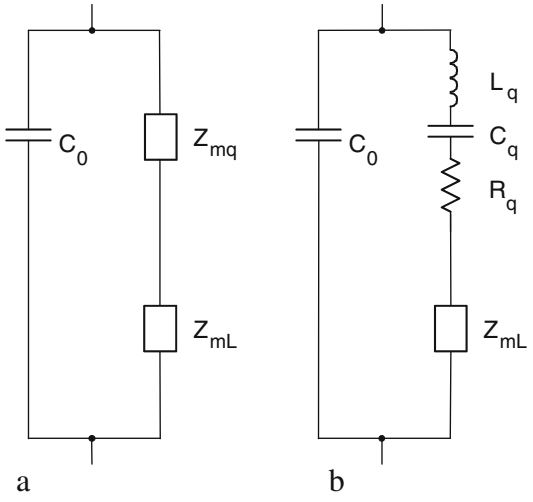

Fig. 5 Presentation of the transmission line model of a quartz crystal in a modified equivalent circuit (**a**) and the modified Butterworth–Van Dyke equivalent circuit (**b**). Z_{mq} represents the motional impedance of the quartz crystal, Z_{mL} is the electrical representation of Z_L

magnitude or zero-phase crossing of the phase. The only straightforward resonant frequency is the maximum of the real part of the electrical admittance, also called in-phase admittance or conductance. The respective frequency, f_s, is the resonant frequency of the motional arm. Zero-phase oscillators require compensation of C_0 to be applicable. Near resonance of the quartz crystal Z_{mq} can be presented as equivalent circuit elements C_q, L_q and R_q, arranged as a serial resonant circuit. One obtains the modified Butterworth–Van Dyke equivalent circuit, Fig. 5b, e.g. Refs. [156, 162]. The complex element Z_{mL} can be separated into a frequency-independent resistance and inductance only in certain circumstances, e.g. for a Newtonian liquid.

6. Z_L is a complex value. The imaginary part of the acoustic load governs the changes in the serial resonant frequency [155], in most sensor applications the values are proportional:

$$\frac{\Delta f_s}{f0} \infty - \mathrm{Im}(Z_L) \tag{1}$$

7. The real part of the acoustic load describes acoustic energy loss within the layer(s). It can be represented by changes in the resistance of the serial branch of the equivalent circuit of the sensor e.g. Ref. [160], bandwidth [155] or a dissipation factor [163].

$$\Delta R \infty \mathrm{Re}(Z_L) \tag{2}$$

8. Behling [164] introduced notation for the acoustic load which clearly depicts its character. He separated a mass factor M and an acoustic factor, V

$$Z_L = \mathrm{j}M \cdot V \tag{3}$$

where

$$M = \omega\rho h \tag{4a}$$

$$V = \frac{\tan\varphi}{\varphi} \tag{4b}$$

ρ is the density, h is the thickness of the coating, φ is the phase shift the acoustic wave undergoes while traveling through the film and $\omega=2\pi f$ is the angular frequency, f the resonant frequency, $\mathrm{j} = \sqrt{-1}$.

9. With the notation of Eq. 4a and 4b one can distinguish four regimes in which a QCR can work, Table 1. V=1 represents the pure gravimetric response, the classical microbalance principle. In all other cases so-called non-gravimetric effects contribute to the sensor response.

Table 1 Types of non-gravimetric regime

Case 1	$M \rightarrow M+\mathrm{d}M$	V=1	⇒	Gravimetric sensor
Case 2	$M \rightarrow M+\mathrm{d}M$	$V \approx \mathrm{const} > 1$	⇒	Acoustically amplified gravimetric sensor
Case 3	$M \rightarrow M+\mathrm{d}M$	$V \rightarrow V \pm \mathrm{d}V$	⇒	Mass and material effect sensor
Case 4	$M \approx \mathrm{const}$	$V \rightarrow V \pm \mathrm{d}V$	⇒	Film properties sensor

They are called non-gravimetric because the phase shift and hence the acoustic factor contains material properties of the coating:

$$\varphi = \frac{M}{Z_c} \tag{5}$$

10. $Z_c = \sqrt{\rho G}$ is the characteristic impedance of the coating material and should not be confused with the acoustic load. G is the shear modulus and a complex value (except for pure elastic materials, for which G is real, and pure viscous (Newtonian) liquids, for which $G = \mathrm{j}\omega\eta_l$ is imaginary; η_l is the viscosity).
11. For a complex shear modulus, G, the acoustic factor is also complex: $V = V' + \mathrm{j}V''$, whereas M remains real. Consequently Z_L becomes:

$$Z_L = Z_L^{'} + \mathrm{j}Z_L^{''} = -MV^{''} + \mathrm{j}MV^{'} \tag{6}$$

V' can be understood as acoustic amplification of the mass effect. MV" is always a viscoelastic contribution to acoustic energy dissipation and hence to R; a pure mass does not change R.

12. Behling's notation can also be applied to a two-layer arrangement, e.g. a film covered with a liquid:

$$Z_L = \mathrm{j}(M_1V_1 + M_2V_2)V_M \tag{7}$$

where $V_M = \left(1 - M_1V_1M_2V_2/Z_{c1}^2\right)^{-1}$ is the mixed acoustic factor [165]. The additive character of the contributions of both layers is given only for $V_M = 1$, i.e., $Z_{c1} >> M_1V_1M_2V_2$ which usually requires a large G for the first film.

The gravimetric regime, Table 1 case 1, is obviously the simplest way of exploiting the capabilities of acoustic microsensors. The proof that indeed V=1 is not that simple, as stated below. The shift in frequency because of absorption or adsorption of species can be directly related to the mass accumulated—in principle even without calibration (device characteristics must be known). Under real conditions the electrical and acoustic properties of the transducer in the actual measurement arrangement must be determined. This is especially true for liquid applications, in which surface roughness (liquid trapping), sensor sealing (stress genera-

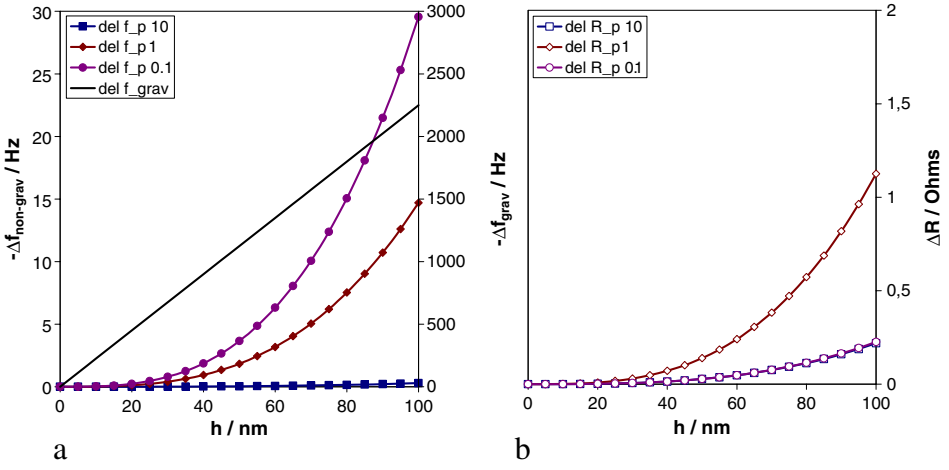

Fig. 6 Gravimetric frequency shift (**a**, *right axis*) and signature of viscoelastic contributions to the sensor response (**a**, *left axis*, and **b**) of a single rubbery film (G'=1 MPa) and a loss factor $\tan\delta$=10, 1, and 0.1, respectively (see *legend*). The resonant frequency is 10 MHz

tion, spurious modes), and the properties of the sensor electronics (phase stability, capacitance compensation) introduce unwanted variances in the sensor transfer function. Unfortunately, many authors stick to frequency changes and consequently do not report on calibration issues. It is not surprising that absolute values differ for similar experiments from one laboratory to another. One can expect helpful information from a ring experiment to extend the large success of acoustic microsensors in laboratory applications to the sensor market.

The second issue is sensor sensitivity which is limited in the gravimetric regime and cannot compete with optical methods such as SPR. Although MEMS-based sensors can significantly improve sensor sensitivity, the signal-to-noise-ratio limitation because of a low Q-factor persists.

Challenges from non-gravimetric effects

Effect of single-film viscoelasticity

Viscoelastic materials are characterized by a complex shear modulus. G of macromolecular materials (including biomolecules) may vary between 10^4 Pa and 10^9 Pa. Rigid or glassy materials have a storage modulus, G', larger than 10^8 Pa and a loss modulus, G'', which is an order of magnitude smaller. Rubbery materials have a modulus of approximately 10^6 Pa, or smaller. A large variety of material property combinations is conceivable. For analysis of acoustic consequences variation of the loss factor $0.1 \leq \tan\delta = G''/G' \leq 10$ is sufficient.

In chemical and biochemical sensing the chemically sensitive film is usually thin and the phase shift the acoustic wave undergoes is small (φ usually smaller than 0.2). In these circumstances the approximation $\varphi = \varphi + \varphi^3/3$ can be applied to Eqs. 1, 2, 3, 4a and 4b. It results in [155, 163, 164]:

$$Z_L = \mathrm{j}M\left(1 + \frac{1}{3}\frac{M^2}{Z_{c1}^2}\right) \tag{8}$$

$$\Delta f \propto MV' = M\left(1 + \frac{1}{3}\frac{J'}{\rho}M^2\right) \tag{9a}$$

$$\Delta R \propto -MV' = M\left(\frac{1}{3}\frac{J''}{\rho}M^2\right) \tag{9b}$$

introducing the compliance with $J' = G'/(G'^2 + G''^2)$ and $J'' = G''/(G'^2 + G''^2)$. The viscoelastic contribution to the frequency shift, i.e. the second term in the brackets in Eq. 9a, depends on M^2, i.e., it depends on the film thickness and, consequently, vanishes for very thin films. In the following treatment we apply the TLM to a 10-MHz AT-cut quartz crystal with an electrode diameter of 6 mm and material properties typical of those of macromolecular substances and a film thickness range also typical of chemical and biosensors. Therefore this and the following diagrams should be understood as a signature of the sensor response [165]. Figure 6a shows, on the right ordinate, the gravimetric response to a single rubbery film facing air vs. the thickness of the layer and, on the left ordinate, the viscoelastic contribution to the sensor response. Compared with the gravimetric response the non-gravimetric contribution to the frequency shift is very small for the conditions selected. Figure 6b shows the resistance increase because of viscoelasticity. It is almost negligible.

Effect of the viscoelasticity of a single film facing a liquid

We replicate the same analysis but now the viscoelastic film faces a liquid, here water. Repeating the above

mathematical treatment, also applying the approximation: $1/(1-x) \approx 1+x$ results in:

$$\Delta f \propto M\left(1 - 2L^2\frac{J''}{\rho}\right) \tag{10a}$$

$$\Delta R \propto M\left(2L^2\frac{J'}{\rho}\right) \tag{10b}$$

L replaces $(\omega\rho_l\eta_l/2)^{1/2}$ and summarizes liquid properties. Note the negative sign in Eq. 10a as opposed to Eq. 9a. Kasemo called this effect "missing mass" [169]. Furthermore, V does not depend on the mass factor. Hence this term appears even for very thin films. The poor quality of the above approximations with increasing film thickness can be improved with an additive term within the brackets linearly dependent on M : $\Delta f : L\frac{J'-J''}{\rho}M$, $\Delta R : 2L\frac{J'+J''}{\rho}M$. The sign of the extension term of Eq. 10a depends on the loss factor. It vanishes with $\tan\delta = 0$ and is positive for materials with $\tan\delta < 1$, thereby compensating the missing mass effect with increasing film thickness. The resistance always increases, in contrast with the behavior of the frequency shift.

Figure 7 reflects these properties. The slope of the viscoelastic contribution to the frequency shift is negative in two cases. This contribution does not vanish even for very thin films. The absolute values are significantly larger, although still small compared with the gravimetric frequency shift (Fig. 6a). The resistance increase is more pronounced. Finally, the contribution to the frequency shift of the elastic film in water has a negative slope for very small h but it becomes positive with increasing h and the "extra mass" value exceeds the value in air for larger film thickness.

Interfacial effects

Interfacial effects related to material properties near the surface which are different from bulk properties can be treated by introducing sub-layers. Interfacial slip [170–179], a violation of the continuity assumption, can also be modeled in this manner. The general acoustic understanding of interfacial phenomena is the appearance of a phase shift, φ_{int} and a characteristic "interfacial" impedance [174]. Figure 8 shows the signature of a (hypothetical) water-like interfacial layer with two different elastic components. Viscous and elastic behavior may arise, for example, if the interfacial layer consists of molecularly distributed water molecules and linker molecules. Other interfacial arrangements are conceivable [180–184]. The effect of an interfacial layer on the frequency shift can be remarkable in a liquid environment and does not depend very much on the shear modulus of the film above. A soft film with a shear modulus of $G'=G''=1$ MPa would respond almost similarly to the glassy film, except that the viscoelastic contribution shown in Fig. 7a would appear as an offset. For comparison, the appearance of an interfacial layer in air is almost negligible.

Changes in viscoelasticity and interfacial properties

Deviations from the gravimetric response are measurable and perhaps useful for viscoelastic amplification of the mass effect—Table 1 case 2. Arrangements for this purpose have been analyzed elsewhere [165]. Sufficient reproducibility is difficult to achieve, because of unavoidable experimental variations and uncertainties in film thickness or surface coverage. In particular, R (or any other value reflecting damping) has other sources than viscosity and tends to vary from one sensor to the next.

A more interesting aspect of a chemical or biochemical experiment is, however, the response of the sensor after interaction of a specific molecule with an already existing film [168]. Now dZ_L is of interest:

$$dZ_L = \frac{\partial Z_L}{\partial M}dM + \frac{\partial Z_L}{\partial V}dV \tag{11a}$$

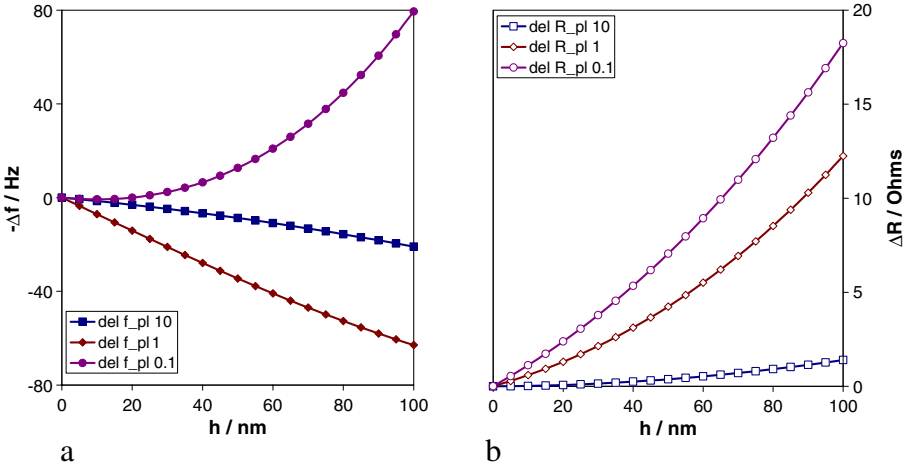

Fig. 7 Signature of the viscoelastic contribution of the same film as in Fig. 6, but the film now faces water. The gravimetric contribution and the contribution of water to the sensor response have been subtracted

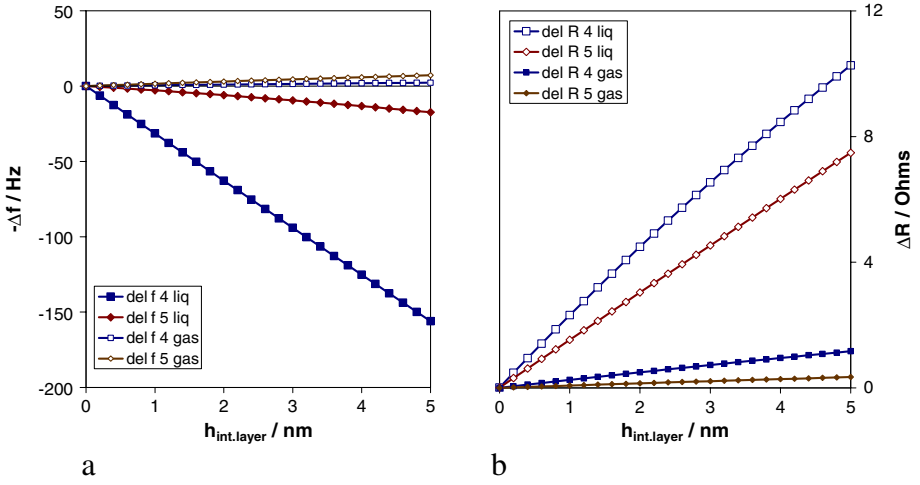

Fig. 8 Signature of an interfacial layer at a solid–solid interface (quartz crystal macromolecular film) with $G'=10^4$ Pa or 10^5 Pa, exponent see legend, and $G''=10^{4.8}$ Pa, equivalent to a viscosity of 1 cP at the resonant frequency of 10 MHz. The film is rigid and has a shear storage modulus $G'=1$ GPa and a shear loss modulus $G''=0.1$ GPa. The film faces air (gas) or is covered with water (liq).The overall thickness of the film and interfacial layer has been kept constant at 50 nm. The gravimetric contribution of the primary film (50 nm) and the contribution of water to the sensor response have been subtracted

with

$$dV \approx \frac{\partial V}{\partial M} dM + \frac{\partial V}{\partial G} dG \qquad (11b)$$

The second term in Eq. 11a cannot be neglected, because of changes in the shear modulus, whereas density changes do not play a recognizable role and are therefore omitted in Eq. 11b. Eq. 11a and 11b result in a viscoelastic contribution to the frequency shift of a single film (Eq. 9a) which is already three times larger even with dG=0.

Table 1 case 2 is difficult to distinguish from case 1, at least for gas sensors. Within experimental error one obtains almost linear dependence of the frequency shift on analyte concentration and the resistance increase is still not obvious. If viscoelastic contributions to the frequency shift are not noticed, calculated primary values, for example accumulated mass, or secondary values, for example partition coefficients, are too large if Sauerbrey's equation has been used.

Table 1 case 3 leads to a means of characterizing the materials of thin polymer films or, remembering the small penetration depth of shear waves in liquids, the interfacial properties of liquids, for example in lubrication or nanotribology [185–195].

Table 1 case 4 is most challenging, because biochemical problems are often related to small molecules, e.g. an enzyme interacting with a large protein. This interaction can change the conformation of the protein, which is accompanied by a modulus change, as is required for case 4. The extreme sensitivity of acoustic microsensors is because the shear modulus can easily vary by an order of magnitude or more. Changes of refractive index are, in contrast, in the percentage range. This is an outstanding trait which makes acoustic sensors extremely versatile in all applications in which the stiffness of thin layer(s) may change. The huge potential of case 4 is about to be discovered for biosensors [196–199]. In case 4 the sensor acts almost purely non-gravimetrically. In this case, with an almost constant mass factor, M, both Δf and ΔR will change because of changes in G', G'', and/or tan δ.

A similar sensor signal may have its origin in interfacial property changes. The non-gravimetric contributions of an interfacial layer may exceed viscoelastic contributions. Although one would not expect large changes in the thickness of an interfacial layer, large frequency and resistance changes can be expected, because of changes in the elastic properties of this layer, as is obvious when moving between the curves in Fig. 8. Note, that interfacial contributions can be constructive or opposite to viscoelastic contributions. It depends very much on the actual viscoelastic properties of both the interfacial layer and the thin film and how they change. These interfacial effects would, however, not appear when using cantilever-like sensors. Longitudinal waves do not probe apparent shear elasticity of an interfacial layer as analyzed above. Incompressibility of the interfacial liquid would dominate.

Prediction of sensor signals as illustrated by Figs. 6–8 is quite helpful; analysis of experimental results is much more involved. As discussed above, the sensor signal just depends on two quantities—the real and imaginary part of the acoustic load. The number of unknowns, even in the simplest case of a single film in air, is four and it increases the more complicated the model becomes. Care must be taken if literature values, usually bulk material properties, are used. The values may differ for thin films or at high probing frequencies. One way to expand the number of independent experimental data is to perform measurements also at overtones of the resonator [200–203]; the frequency dependence of G must also be taken into account, however [204].

Other sensor signal sources

Nuisances are encountered in real experimental arrangements; these nuisances cannot be treated with simple theoretical models. Some work has been published dealing with surface roughness [205–208], stress [209], non-uniformity [210], or compressional waves [211–216]. A major concern is that these factors tend to be affected by the experiment and, therefore, contribute to the measurement signal in an uncontrolled manner. Generalization of acoustic characteristics enables partial treatment within the TLM [217].

Acoustoelectric effects, also, have not yet been considered. Electrode geometry, electrode polarity, fringing fields, and liquid conductivity or liquid permittivity affect the performance of quartz crystal resonator sensors operating in electrolytes and solutions. Electroacoustic effects result from acoustic wave propagation on SAW-like sensors. Here the acoustic wave propagates along the surface of a piezoelectric crystal and interacts also via the associated electrical fields with the overlayer and probes the electrical properties of the material, e.g. the permittivity of the film or the adjacent liquid. For example, the conductivity of the film gives rise to an additional decrease in acoustic wave velocity and to a peak in attenuation [218]. To take advantage of acoustoelectric effects with quartz crystals specific electrode geometry is required [219–223]. A specific version is lateral field excitation [224–227].

Perspectives

There is, understandably, continuing interest in gravimetric acoustic sensors. Their principle of detection is the simplest. Molecular weight is surely a fundamental property of species; therefore, to name two advantages, it does not require any charge transfer or specific labeling. Many acoustic sensors work well in viscous liquids and optically opaque media. The technique is quite easy to use and the equipment required is inexpensive. The sensitivity, however, is limited and cannot compete with that of optical methods, e.g. SPR, and so the gravimetric acoustic principle has a better chance of being applied in simple sensors than in scientific instrumentation. Improvement of sensitivity by use of additional sensor-system elements has been achieved with pre-concentrators and selectivity has been improved by use of chromatography. The range of sensor applications is broad; more applications can be expected for liquid systems, e.g. detection of water pollutants and health monitoring, for which competition from other sensor principles is smaller. Liquid applications require further improvements in sensor-system design to enable their use by unskilled persons also. Contactless magnetic excitation is a promising technique for simplifying handling and overcoming the restriction to piezoelectric materials for resonators but needs further improvement of energy-transfer efficiency. Micromachined sensors, including the development of sensor arrays adapted to robots used in high-throughput technology, overcome the lack of integration potential of classical acoustic devices. The development of these is just beginning. One can expect the necessary improvements, especially in the Q-factor, from vibration modes not common for (atomic) force sensors. Sensitivity to mechanical damage must also be addressed.

Sensor applications also require improved sensor-to-sensor reproducibility, to reduce calibration effort. In practice, frequency measurement before use should be sufficient. Even a reference measurement with a reference substance makes measurement more involved and increases cost; this is acceptable in special cases only. Because reproducibility depends mainly on the reproducibility of the coating procedure, commercially pre-functionalized sensors may lead to an increase in market confidence in acoustic microsensors.

Non-gravimetric acoustic sensors are a much greater challenge. These acoustic sensors can provide measurement capabilities not available with other methods. The outstanding sensitivity of acoustic wave-based sensors to materials and interfacial properties is still far from being systematically exploited. One reason is the lack of relevant information about those properties. The development of non-gravimetric measurement techniques can positively affect research areas such as polymer characterization or micro/nanotribology and can, especially, boost measurement capabilities in biochemistry or pharmaceutical and biomaterials research. Growing confluence of previously unrelated disciplines is required. Miniaturization on micro and nanoscales, array technology, and improvements in signal-transduction mechanisms combined with information processing has created a rapidly developing field of measurement technology. The theory of acoustic wave propagation can be used to predict sensor response to material, interfacial, and other properties, further effects, for example mass point contact, are about to be described. It is now necessary to develop better models of the (bio) systems themselves, probably on the level of molecular dynamics. Improvements in preparation technology enable access to systematic variation of acoustically relevant properties. Finally, other measurement technology [228–235] must be simultaneously applied to reduce the number of unknowns of the systems under investigation.

References

1. Sauerbrey G (1959) Verwendung von Schwingquarzen zur Wägung dünner Schichten und zur Mikrowägung. Zeitschrift Physik 155:206–212
2. EerNisse EP, Wiggins RB (2001) Review of thickness-shear mode quartz resonator sensors for temperature and pressure. IEEE Sensors J 1:79–87
3. King WH Jr (1964) Piezoelectric sorption detector. Anal Chem 36:1735–1739
4. Ward MD, Buttry DA (1990) In situ interfacial mass detection with piezoelectric transducers. Science 249:1000–1007
5. Prajakovic LV, Cavic-Vlasal BA, Ghaemmaghami V, Kallury KMR, Kipling AL, Thompson M (1991) Mediation of acoustic energy transmission from acoustic wave sensors to the liquid phase by interfacial viscosity. Anal Chem 63:615–621

6. Cavic BA, Chu FL, Furtado LM, Ghafouri S, Hayward GL, Mack DP, McGovern ME, Su H, Thompson M (1997) Acoustic waves and the real-time study of biochemical macromolecules at the liquid/solid interface. Faraday Discuss 107:159–176
7. Eichelbaum F, Borngräber R, Schröder J, Lucklum R, Hauptmann P (1999) Interface circuits for quartz crystal-microbalance sensors. Rev Sci Instr 70:2537–2545
8. Kanazawa KK (2005) Some basics for operating and analyzing data using the thickness shear mode resonator. Analyst 130:1459–1464
9. Scholl G, Schmidt F, Ostertag T, Reindl L, Scherr H, Wolff U (1998) Wireless passive SAW sensor system for industrial and domestic applications. IEEE Int Freq Cont Symp Proceedings 595–601
10. Springer A, Weigel R, Pohl A, Seifert F (1999) Wireless identification and sensing using surface acoustic wave devices. Mechatronics 9:745–756
11. Dong Y, Cheng W, Wang S, Li Y, Feng G (2001) A multi-resolution passive SAW chemical sensor. Sens Actuators B 76 76:130–133
12. Ballantine DS, White RM, Martin SJ, Ricco AJ, Zellers ET, Frye GC, Wohltjen H (1997) Acoustic Wave Sensors. Academic, London
13. Arnau A (Ed.) (2004) Piezoelectric Transducers and Applications. Springer, Berlin Heidelberg New York
14. Grate JW, Martin SJ, White RM (1993) Acoustic wave microsensors. Anal Chem 65:987A–996A
15. Josse F (1994) Acoustic wave liquid-phase-based microsensors. Sens Actuators A 44:199–208
16. Kaspar M, Stadler H, Weiß T, Ziegler C (2000) Thickness shear mode resonators ("mass-sensitive devices") in bioanalysis. Fresenius J Anal Chem 366:602–610
17. Viens M, Li P, Wang Z, Jen CK, Thompson M, Cheeke JDN (1996) Mass sensitivity of thin rod acoustic wave sensors. IEEE Trans. Ultrason Ferroelec Freq Contr 43:852–857
18. Lin X, Cheeke JDN, Wang Z, Jen CK, Viens M, Yi G, Sayer M (1995) Ultrasonic thin-walled tube wave devices for sensor applications. Appl Phys Lett 76:37–39
19. Li PCH, Thompson M (1996) Mass sensitivity of the tube acoustic wave sensor in the extensional mode. Anal Chim Acta 336:13–21
20. Yamanaka K, Ishikawa S, Nakaso N, Takeda T, Mihara T, Tsukahara Y (2003) Ball SAW devices for hydrogen gas sensor. IEEE Ultrason Symp Proceedings 299–302
21. Huang CL, Tay KW, Wu L (2005) Fabrication and performance analysis of film bulk acoustic wave resonators. Materials Letters 59:1012–1016
22. Dorozhkin LM, Dorozhkina GN, Fokin AV, Rozanov IA, Sabelnikov AG, Sevastjanov VG (2005) Thin film piezoelectric acoustic sensor (TFPAS): further experimental validation of the theory of resonance sensitivity. Sens Actuators B 106:529–533
23. Thundat T, Chen GY, Warmack RJ, Allison DP, Wachter EA (1995) Vapor Detection Using Resonating Microcantilevers. Anal Chem 67:519–521
24. Berger R, Gerber C, Lang HP, Gimzewski JK (1997) Micromechanics: a toolbox for femtoscale science: towards a laboratory on a tip. Microelectron Eng 35:373–379
25. Lack FR, Willard GW, Fair IE (1934) Some improvements in quartz crystal circuit elements. Bell Syst Tech J 13:453–463
26. Ballato AD, Bechmann R (1960) Effect of initial stress on vibrating quartz plates. Proceedings IRE 48:261–262
27. Kosinski JA, Pastore RA (2001) Theory and design of piezoelectric resonators immune to acceleration: present state of the art. IEEE Trans Ultrason Ferroel Freq Contr 48:1426–1437
28. Tancrell RH, Schulz MB, Barrett HH, Davies L, Holland MG (1969) Dispersive delay lines using ultrasonic surface waves. Proceedings IEEE 57:1211–1213
29. Dieulesaint E, Hartmann P (1973) Acoustic surface wave filters. Ultrasonics 11:24–30
30. Coon A (1991) SAW Filters and Competitive Technologies-A Comparative Review IEEE Ultrason Symp Proceedings 155–160
31. Aigner R MEMS in RF-Filter Applications: Thin Film Bulk-Acoustic-Wave Technology 13. Int Conf Solid-State Sensors Actuators Microsyst (Transducers '05) to be published in Sensors Actuators
32. Binning G, Quate CF, Gerber C (1986) Atomic Force Microscope. Phys Rev Lett 56:930–933
33. Bard AJ, Fan FRF, Kwak J, Lev O (1989) Scanning electrochemical microscopy. Introduction and principles. Anal Chem 61:132–138
34. Bykov VA, Novikov YA, Rakov AV, Shikin SM (2003) Defining the parameters of a cantilever tip AFM by reference structure. Ultramicroscopy 96:175–180
35. Fasching RJ, Tao Y, Prinz FB (2005) Cantilever tip probe arrays for simultaneous SECM and AFM analysis. Sensors Actuators: B 108:964–972
36. Lin Z, Yip CM, Joseph IS, Ward MD (1993) Operation of an ultrasensitive 30 MHz quartz crystal microbalance in liquids. Anal Chem 65:1546–1551
37. Abe T, Esashi M (2000) One-chip multichannel quartz crystal microbalance (QCM) fabricated by Deep RIE. Sens Actuators A 82:139–143
38. Vig JR, Filler RF, Kim Y (1995) Microresonator sensor array. IEEE Int Freq Contr Symp Proceedings 852–869
39. Zimmermann B, Lucklum R, Hauptmann P, Rabe J, Büttgenbach S (2001) Electrical characterisation of high frequency thickness-shear-mode resonators by impedance analysis. Sensor Actuators B 76:47–57
40. Rabe J, Büttgenbach S, Schröder J, Hauptmann P (2003) Monolithic Miniaturized Quartz Microbalance Array and Its Application to Chemical Sensor Systems for Liquids. IEEE Sensors J 3:361–368
41. Stevenson AC, Lowe CR (1998) Noncontact excitation of high Q acoustic resonances in glass plates. Appl Phys Lett 73:447–449
42. Stevenson AC, Lowe CR (1999) Magnetic-acoustic-resonator sensors (MARS): a new sensing technology. Sens Actuators A 72:32–37
43. Lucklum F, Hauptmann P, deRooij NF accepted for Meas Sci Technol
44. Thompson M, Ballantyne SM, Stevenson AC, Lowe CR (2003) Electromagnetic excitation of high frequency acoustic waves and detection in the liquid phase. Analyst 128:1048–1055
45. Vasilescu A, Ballantyne SM, Cheran LE, Thompson M (2005) Surface properties and electromagnetic excitation of a piezoelectric gallium phosphate biosensor. Analyst 130:213–220
46. Darinskii AN unpublished
47. Stevenson AC, Araya-Kleinsteuber B, Sethi RS, Metha HM, Lowe CR (2003) The acoustic spectrophonometer: a novel bioanalytical technique based on multifrequency acoustic devices. Analyst 128:1222–1227
48. Ballantyne SM, Thompson M (2004) Superior analytical sensitivity of electromagnetic excitation compared to contact electrode instigation of transverse acoustic waves. Analyst 129:219–224
49. Stevenson AC, Araya-Kleinsteuber B, Sethi RS, Metha HM, Lowe CR (2005) Planar coil excitation of multifrequency shear wave transducers. Biosens Bioelectron 20:1298–1304
50. Raiteri R, Grattarola M, Butt HJ, Skládal P (2001) Micromechanical cantilever-based biosensors. Sens Actuators B: 79:115–126
51. Ziegler C (2004) Cantilever-based biosensors. Anal Bioanal Chem 379:946–959
52. Lang HP, Hegner M, Gerber C (2005) Cantilever array sensors. Materials Today 8:30–36
53. Wang Z, Yue R, Zhang R, Liu L (2005) Design and optimization of laminated piezoresistive microcantilever sensors. Sens Actuators A 120:325–336

54. Adams JD, Rogers B, Manning L, Hu Z, Thundat T, Cavazos H, Minne SC (2005) Piezoelectric self-sensing of adsorption-induced microcantilever bending. Sens Actuators A 121:457–461
55. Zribi A, Knobloch A, Tian WC, Goodwin S (2005) Micro-machined resonant multiple gas sensor. Sens Actuators A 122:31–38
56. Tian F, Hansen KM, Ferrell TL, Thundat T (2005) Dynamic Microcantilever Sensors for Discerning Biomolecular Interactions. Anal Chem 77:1601–1606
57. Zribi A, Knobloch A, Rao R (2005) CO_2 detection using carbon nanotube networks and micromachined resonant transducers. Appl Phys Lett 86:203112–20115
58. Mukhopadhyay R, Lorentzen M, Kjems J, Besenbacher F Nanomechanical Sensing of DNA Sequences Using Piezoresistive Cantilevers. Langmuir ASAP Article S0743–7463(05) 01168–6
59. Campbell GA, Mutharasan R (2005) Detection of pathogen *Escherichia coli* O157:H7 using self-excited PZTglass microcantilevers. Biosens Bioelectron 21:462–473
60. Gfeller KY, Nugaeva N, Hegner M (2005) Micromechanical oscillators as rapid biosensor for the detection of active growth of Escherichia coli. Biosens Bioelectron 21:528–533
61. Agostona A, Keplinger F, Jakoby B (2005) Evaluation of a vibrating micromachined cantilever sensor for measuring the viscosity of complex organic liquids. Sens Actuators A 123–124:82–86
62. Lee Y, Lim G, Moon W (2005) A piezoelectric micro-cantilever bio-sensor using the mass-microbalancing technique with self-excitation 13. Int Conf Solid-State Sensors Actuators Microsyst (Transducers 05) Proceedings 644–647
63. Vancura C, Ruegg M, Li Y, Hagleitner C, Hierlemann A (2005) Magnetically actuated complementary metal oxide semiconductor resonant cantilever gas sensor systems. Anal Chem 77:2690–2699
64. Han LH, Chen S (2005) Wireless bimorph micro-actuators by pulsed laser heating. Sens Actuators A 121:35–43
65. Lin YC, Ono T, Esashi M (2005) Quartz-crystal cantilevered resonator for nanometric sensing 13. Int Conf Solid-State Sensors Actuators Microsyst (Transducers 05) Proceedings 593–596
66. Vidic A, Then D, Ziegler C (2003) A new cantilever system for gas and liquid sensing. Ultramicroscopy 97:407–416
67. Zhang W, Turner KL (2005) Application of parametric resonance amplification in a single-crystal silicon microoscillator based mass sensor. Sens Actuators A 122:23–30
68. Dohn S, Sandberg R, Svendsen W, Boisen A (2005) Enhanced functionality of cantilever based mass sensors using higher modes and functionalized particles 13. Int Conf Solid-State Sensors Actuators Microsyst (Transducers 05) Proceedings 636–639
69. Vancura C, Li Y, Kirstein KU, Josse F, Hierlemann A, Lichtenberg J (2005) Fully integrated CMOS resonant cantilever sensor for biochemical detection in liquid environments 13. Int Conf Solid-State Sensors Actuators Microsyst (Transducers 05) Proceedings 640–643
70. Seo JH, Brand O (2005) Novel high Q-factor resonant microsensor platform for chemical and biological applications 13. Int Conf Solid-State Sensors Actuators Microsyst (Transducers 05) Proceedings 247–251
71. Burg TB, Manalis SR (2003) Suspended microchannel resonators for biomolecular detection. Appl Phys Lett 83:2698–2700
72. Ferrari V, Marioli D, Taroni A (2001) Theory, modeling and characterization of PZT-on-alumina resonant piezo-layers as acoustic-wave mass sensors. Sens Actuators A 92:182–190
73. Schreiter M, Gabl R, Pitzer D, Primig R, Wersing W (2004) Electro-acoustic hysteresis behaviour of PZT thin film bulk acoustic resonators. J European Ceramic Soc 24:1589–1592
74. Ferrari M, Ferrari V, Marioli D, Taroni A, Suman M, Dalcanale E (2004) Cavitand-coated PZT resonant piezo-layer sensors: properties, structure, and comparison with QCM sensors at different temperatures under exposure to organic vapors. Sens Actuators B 103:240–246
75. Kang YR, Kang SC, Paek KK, Kim YK, Kim SW, Ju BK (2005) Air-gap type film bulk acoustic resonator using flexible thin substrate. Sens Actuators A 117:62–70
76. Nicu L, Guirardel M, Chambosse F, Rougerie P, Hinh S, Trevisiol E, Francois JM, Majoral JP, Caminade AM, Cattand E, Bergaud C (2005) Resonating piezoelectric membranes for microelectromechanically based bioassay: detection of streptavidin-gold nanoparticles interaction with biotinylated DNA. Sens Actuators B 110:125–136
77. Huang CL, Tay KW, Wu L (2005) Fabrication and performance analysis of film bulk acoustic wave resonators. Materials Lett 59:1012–1016
78. Hauptmann P, Hoppe N, Püttmer A (2002) Application of ultrasonic sensors in the process industry. Meas Sci Technol 13: R73–R83
79. Püttmer A, Linzenkirchner E, Hauptmann P (2004) Ultraschallsensoren für die Prozesstechnik. atp 46:S51–S59
80. Ladabaum I, Khuri-Yakub BT, Spoliansky D (1996) Micromachined ultrasonic transducers (MUTs): 11.4 MHz transmission in air and More. Appl Phys Lett 68:7–9
81. Eccardt P, Niederer K, Scheiter T, Hierold C (1996) IEEE Ultrason Symp Proceedings vol. 2:959–962
82. Jin X, Ladabaum I, Khuri-Yakub BT (1998) The microfabrication of capacitive ultrasonic transducers. IEEE J Microelectromech Syst 7:295–302
83. Bayram B, Oralkan O, Ergun AS, Haeggstrom E, Yaralioglu GG, Khuri-Yakub BT (2005) Capacitive micromachined ultrasonic transducer design for high power transmission. IEEE Trans Ultrason Ferroelec Freq Contr 52:326–339
84. Huang Y, Haeggstrom EO, Zhuang X, Ergun AS, Khuri-Yakub BT (2005) A solution to the charging problems in capacitive micromachined ultrasonic transducers. Trans Ultrason Ferroelec Freq Contr 52:578–580
85. Caliano G, Savoia A, Caronti A, Foglietti V, Cianci E, Pappalardo M (2005) Capacitive micromachined ultrasonic transducer with an open-cells structure. Sens Actuators A 121:382–387
86. Guldiken RO, Degertekin FL (2005) Micromachined capacitive transducer arrays for intravascular ultrasound imaging MEMS Proceedings 315–318
87. Perçin G, Atalar A, Levent Degertekin F, Khuri-Yakub BT (1998) Micromachined two-dimensional array piezoelectrically actuated transducers. Appl Phys Lett 72:1397–1399
88. http://piezo.stanford.edu/library/papers/chan2.pdf
89. Santos JP, Fernández MJ, Fontecha JL, Lozano J, Aleixandre M, García M, Gutiérrez J, Horrillo MC (2005) SAW sensor array for wine discrimination. Sens Actuators B 107:291–295
90. Atashbar MZ, Bejcek B, Vijh A, Singamaneni S (2005) QCM biosensor with ultra thin polymer film. Sens Actuators B 107:945–951
91. Matsuguchi M, Kadowaki Y, Tanaka M (2005) A QCM-based NO_2 gas detector using morpholine-functional cross-linked copolymer coatings. Sens Actuators B 108:572–575
92. Razan F, Zimmermann C, Rebière D, Déjous C, Pistré J, Destarac M, Pavageau B (2005) Radio frequency thin film characterization with polymer-coated Love-wave sensor. Sens Actuators B 108:917–924
93. Rahman MA, Kwon NH, Won MS, Sang Choe E, Shim YB (2005) Functionalized Conducting Polymer as an Enzyme-Immobilizing Substrate: an amperometric glutamate microbiosensor for in vivo measurements. Anal Chem ASAP Article 10.1021
94. Sellborn A, Andersson M, Hedlunda J, Andersson J, Berglin M, Elwing H (2005) Immune complement activation on polystyrene and silicon dioxide surfaces, Impact of reversible IgG adsorption. Mol Immunology 42:569–574

95. Horkay F, Horkayne-Szakaly I, Basser PJ (2005) Measurement of the osmotic properties of thin polymer films and biological tissue samples. Biomacromolecules 6:988–993
96. Kim SR, Kim JD, Choi KH, Chang YH (1997) NO2-sensing properties of octa(2–ethylhexyloxy)metallophthalocyanine LB films using quartz-crystal microbalance. Sens Actuators B 40:39–45
97. Penza M, Cassano G, Sergi A, Sterzo Lo C, Russo MV (2001) SAW chemical sensing using poly-ynes and organometallic polymer films. Sens Actuators B 81:88–98
98. Jakubik WP, Urbaczyk MW, Kochowski S, Bodzenta J (2003) Palladium and phthalocyanine bilayer films for hydrogen detection in a surface acoustic wave sensor system. Sens Actuators B 96:321–328
99. Ricco AJ, Crooks RM, Osbourn GC (1998) Surface acoustic wave chemical sensor arrays: new chemically sensitive interfaces combined with novel cluster analysis to detect volatile organic compounds and mixtures. Accounts Chem Research 31:289–296
100. Heila C, Windscheif GR, Braschohs S, Flörke J, Gläser J, Lopez M, Müller-Albrecht J, Schramm U, Bargon J, Vögtle F (1999) Highly selective sensor materials for discriminating carbonyl compounds in the gas phase using quartz microbalances. Sens Actuators B 61:51–58
101. Schlupp M, Weil T, Berresheim AJ, Wiesler UM, Bargon J, Müllen K (2001) Polyphenylen-Dendrimere als empfindliche und selektive Sensorschichten. Angew Chem 113:4124–4129
102. Zhao H, Li J, Xi F, Jiang L (2004) Polyamidoamine dendrimers inhibit binding of Tat peptide to TAR RNA. FEBS Lett 563:241–245
103. Koshets IA, Kazantseva ZI, Shirshov YM, Cherenok SA, Kalchenko VI (2005) Calixarene films as sensitive coatings for QCM-based gas sensors. Sens Actuators B: 106:177-181
104. Ersöz A, Denizli A, Özcan A, Say R (2005) Molecularly imprinted ligand-exchange recognition assay of glucose by quartz crystal microbalance. Biosens Bioelectron 20:2197–2202
105. Piacham T, Josell Å, Arwin H, Prachayasittikul V, Ye L (2005) Molecularly imprinted polymer thin films on quartz crystal microbalance using a surface bound photo-radical initiator. Anal Chim Acta 536:191–196
106. Rick J, Chou TC (2005) Imprinting unique motifs formed from protein-protein associations. Anal Chim Acta 542:26–31
107. Feng L, Liu Y, Zhou X, Hu J (2005) The fabrication and characterization of a formaldehyde odor sensor using molecularly imprinted polymers. J. Colloid Interface Sci 284:378–382
108. Ebarvia BS, Cabanilla S, Sevilla F III (2005) Biomimetic properties and surface studies of a piezoelectric caffeine sensor based on electrosynthesized polypyrrole. Talanta 66:145–152
109. Lee SW, Yang DH, Kunitake T (2005) Regioselective imprinting of anthracenecarboxylic acids onto TiO_2 gel ultrathin films: an approach to thin film sensor. Sens Actuators B 104:35–42
110. Zhang Z, Li H, Liao H, Nie L, Yao S (2005) Influence of cross-linkers' amount on the performance of the piezoelectric sensor modified with molecularly imprinted polymers. Sens Actuators B 105:176–182
111. Ebarvia BS, Sevilla F III (2005) Piezoelectric quartz sensor for caffeine based on molecularly imprinted polymethacrylic acid. Sens Actuators B 107:782–790
112. Reddy S, Stevenson D, Hawkins DM Molecular Imprinting of Proteins in Hydrogels. Possibilities for Novel Sensing of Biomolecules. Biosensor & Biomaterials Workshop 2005, Tsukuba, Japan, to be published in The Analyst
113. Yoshimi Y, Sekine S, Hattori K, Kohori F, Sakai K Gate Effect: biomimetric receptors synthesized by molecular imprinting. Biosensor & Biomaterials Workshop 2005, Tsukuba, Japan, to be published in The Analyst
114. Yang DH, Bae AH, Koumoto K, Lee SW, Sakurai K, Shinkai S (2005) In situ monitoring of polysaccharide-polynucleotide interaction using a schizophyllan-immobilized QCM device. Sens Actuators B 105:490–494
115. Tsai WC, Lin IC (2005) Development of a piezoelectric immunosensor for the detection of alpha-fetoprotein. Sens Actuators B 106:455–460
116. Loergen JW, Kreutz C, Bargon J, Krattiger P, Wennemers H (2005) Diketopiperazine receptors: highly selective layers for gravimetric sensors. Sens Actuators B 107:366–371
117. Boireau W, Zeeh JC, Puig PE, Pompon D (2005) Unique supramolecular assembly of a redox protein with nucleic acids onto hybrid bilayer: towards a dynamic DNA chip. Biosensors, Bioelectron 20:1631–1637
118. Gronewold TM, Glass S, Quandt E, Famulok M (2005) Monitoring complex formation in the blood coagulation cascade using aptamer-coated SAW sensors. Biosens Bioelectron 20:2044–2052
119. Melles E, Anderson H, Wallinder D, Shafqat J, Bergman T, Aastrup T, Jornvall H (2005) Electroimmobilization of proinsulin C-peptide to a quartz crystal microbalance sensor chip for protein affinity purification. Anal Biochem 341:89–93
120. Janshoff A, Steinem C (2005) Label-free detection of protein-ligand interactions by the quartz crystal microbalance. Methods Mol Biol 305:47–64
121. Liu SF, Li JR, Jiang L (2005) Surface modification of platinum quartz crystal microbalance by controlled electrodeless deposition of gold nanoparticles and its enhancing effect on the HS–DNA immobilization. Colloids Surfaces A 257–258:57–62
122. Stengel G, Höök F, Knoll W (2005) Viscoelastic modeling of template-directed DNA synthesis. Anal Chem 77:3709–3714
123. Matsuno H, Furusawa H, Okahata Y (2005) Kinetic studies of DNA cleavage reactions catalyzed by an ATP-dependent deoxyribonuclease on a 27-MHz quartz-crystal microbalance. Biochemistry 44:2262–2270
124. Hur Y, Han J, Seon J, Pak YE, Roh Y (2005) Development of an SH-SAW sensor for the detection of DNA hybridization. Sens Actuators A 120:462–467
125. Mannelli I, Minunni M, Tombelli S, Wang R, Spiriti M, Mascini M (2005) Direct immobilisation of DNA probes for the development of affinity biosensors. Bioelectrochem 66:129–138
126. Tedeschi L, Citti L, Domenici C (2005) An integrated approach for the design and synthesis of oligonucleotide probes and their interfacing to a QCM-based RNA biosensor. Biosens Bioelectron 20:2376–2385
127. Liu S, Liu Y, Li J, Guo M, Nie L, Yao S (2005) Study on the interaction between DNA and protein induced by anticancer drug carboplatin. J Biochem Biophys Methods 63:125–136
128. Alessandrini A, De Renzi V, Berti L, Barak I, Facci P (2005) Chemically homogeneous, silylated surface for effective DNA binding and hybridization. Surface Science 582:202–208
129. Darain F, Park DS, Park JS, Shim YB (2004) Development of an immunosensor for the detection of vitellogenin using impedance spectroscopy. Biosens Bioelectron 19:1245–1252
130. Kurosawa S, Nakamura M, Park JW, Aizawa H, Yamada K, Hirata M (2004) Evaluation of a high-affinity QCM immunosensor using antibody fragmentation and 2-methacryloyloxyethyl phosphorylcholine (MPC) polymer. Biosens Bioelectron 20:1134–1139
131. Bonroy K, Friedt JM, Frederix F, Laureyn W, Langerock S, Campitelli A, Sara M, Borghs G, Declerck B, Goddeeris P (2004) Realization and characterization of porous gold for increased protein coverage on acoustic sensors. Anal Chem 76:4299–4306
132. Su X, Zong Y, Richter R, Knoll W (2005) Enzyme immobilization on poly(ethylene-co-acrylic acid) films studied by quartz crystal microbalance with dissipation monitoring. J Colloid Interface Sci 287:35–42
133. Rick J, Chou TC (2005) Imprinting unique motifs formed from protein-protein associations. Anal Chim Acta 542:26–31

134. Li J, Thielemann C, Reuning U, Johannsmann D (2005) Monitoring of integrin-mediated adhesion of human ovarian cancer cells to model protein surfaces by quartz crystal resonators: evaluation in the impedance analysis mode. Biosens Bioelectron 20:1333–1340
135. Joseph S, Gronewold TMA, Schlensog MD, Olbrich C, Quandt E, Famulok M, Schirner M (2005) Specific targeting of ultrasound contrast agent (USCA) for diagnostic application: an in vitro feasibility study based on SAW biosensor. Biosens Bioelectron 20:1829–1835
136. Skladal P, Jilkova Z, Svoboda I, Kolar V (2005) Investigation of osteoprotegerin interactions with ligands and antibodies using piezoelectric biosensors. Biosens Bioelectron 20:2027–2034
137. Zhang Y, Wang M, Xie Q, Wen X, Yao S (2005) Monitoring of the interaction of tannin with bovine serum albumin by electrochemical quartz-crystal impedance system and fluorescence spectrophotometry. Sens Actuators B 105:454–463
138. Oshima K, Nakajima H, Takahashi S, Kera Y, Shimomura M, Miyauchi S (2005) Quartz crystal microbalance assay for determination of plasma vitellogenin. Sens Actuators B 105:473–478
139. Michalzik M, Wendler J, Rabe J, Büttgenbach S, Bilitewski U (2005) Development and application of a miniaturised quartz crystal microbalance (QCM) as immunosensor for bone morphogenetic protein-2. Sens Actuators B 105:508–515
140. Prachayasittikul V, Na Ayudhya CI, Hilterhaus L, Hinz A, Tantimongcolwat T, Galla HJ (2005) Interaction analysis of chimeric metal-binding green fluorescent protein and artificial solid-supported lipid membrane by quartz crystal microbalance and atomic force microscopy. Biochem Biophys Res Commun 327:174–182
141. Le Guillou-Buffello D, Helary G, Gindre M, Pavon-Djavid G, Laugier P, Migonney V (2005) Monitoring cell adhesion processes on bioactive polymers with the quartz crystal resonator technique. Biomaterials 26:4197–4205
142. Tomchenko AA, Harmer GP, Marquis BT (2005) Detection of chemical warfare agents using nanostructured metal oxide sensors. Sens Actuators B 108:41–55
143. Si SH, Fung YS, Zhu DR (2005) Improvement of piezoelectric crystal sensor for the detection of organic vapors using nanocrystalline TiO2 films. Sens Actuators B 108:165–171
144. Sun H, Zhang YY, Si SH, Zhu DR, Fung YS (2005) Piezoelectric quartz crystal (PQC) with photochemically deposited nano-sized Ag particles for determining cyanide at trace levels in water. Sens Actuators B 108:925–932
145. Wang H, Wu J, Li J, Ding Y, Shen G, Yu R (2005) Nanogold particle-enhanced oriented adsorption of antibody fragments for immunosensing platforms. Biosens Bioelectron 20:2210–2217
146. Mo ZH, Liang YL, Wang HL, Liu FW, Xue YX (2005) Microgravimetric flow analysis of nucleic acid based on adsorption of nanoparticle-bioconjugate. Anal Bioanal Chem 382:996–1000
147. http://www.q-sense.com/
148. Auld BA Acoustic Fields and Waves in Solids vol. 1+2 Krieger Publ. Comp. 1990
149. Tiersten HF (1969) Linear Piezoelectric Plate Vibrations. Plenum, New York
150. Mason WP (1969) Physical Acoustic and the Properties of Solids. Van Nostrand Co.
151. Rosenbaum JF (1988) Bulk Acoustic Wave Theory and Devices. Artech, Boston
152. Nowotny H, Benes E (1970) General one-dimensional treatment of the layered piezoelectric resonator with two electrodes. Electron Lett 6:398–399
153. Krimholtz R, Leedom DA, Matthaei GL (1970) New equivalent circuits for elementary piezoelectric transducers. J Acoust Soc Amer 82:513–521
154. Martin SJ, Granstaff VE, Frye GC (1991) Characterization of a quartz crystal microbalance with simultaneous mass and liquid loading. Anal Chem 63:2272–2281
155. Johannsmann D, Mathauer K, Wegner G, Knoll W (1992) Viscoelastic properties of thin films probed with a quartz-crystal resonator. Phys Rev B 46:7808–7815
156. Granstaff VE, Martin SJ (1994) Characterization of a thickness-shear mode quartz resonator with multiple nonpiezioelectric layers. J Appl Phys 75:1319–1329
157. Martin SJ, Frye GC, Senturia SD (1994) Dynamics and response of polymer-coated surface acoustic wave devices: effect of viscoelastic properties and film resonance. Anal Chem 66:2201–2219
158. Behling C, Lucklum R, Hauptmann P (1998) Response of quartz-crystal resonators to gas and liquid analyte exposure. Sens Actuators A 68:388–398
159. Bandey HL, Martin SJ, Cernosek RW (1999) Modeling the response of thickness-shear mode resonators under various loading conditions. Anal Chem 71:2205–2214
160. Lucklum R, Behling C, Hauptmann P (1999) Role of mass accumulation and iscoelastic film properties for the response of acoustic-wave-based chemical sensors. Anal Chem 71:2488–2496
161. Lucklum R, Hauptmann P (2000) The quartz crystal microbalance: mass sensitivity, viscoelasticity and acoustic amplification. Sens Actuators B 70:30–36
162. Behling C, Lucklum R, Hauptmann P (1997) Possibilities and limitations in quantitative determination of polymer shear parameters by TSM resonators. Sensors and Actuators A 61:260–266
163. Rodahl M, Kasemo B (1996) Frequency and dissipation-factor responses to localized liquid deposits on a QCM electrode. Sens Actuators B 37:111–116
164. Behling C, Lucklum R, Hauptmann P (1998) The nongravimetric quartz crystal resonator response and its application for polymer shear moduli determination. Meas Sci Technol 9:1886–1893
165. Lucklum R, Behling C, Hauptmann P (2001) Signal amplification with multilayer arrangements on chemical quartz-crystal-resonator sensors. IEEE Trans Ultrason Ferroel Freq. Contr 47:1246–1252
166. Dormack A, Prucker O, Rühe J, Johannsmann D (1997) Swelling of a polymer brush probed with a quartz crystal resonator. Phys Rev E 56:680–689
167. Lucklum R, Hauptmann P (2003) Transduction mechanism of acoustic-wave based chemical and biochemical sensors. Meas Sci Technol 14:1854–1864
168. Lucklum R (2005) Non-Gravimetric Contributions to QCR Sensor Response. Analyst 130:1465–1473
169. Voinova MV, Jonson M, Kasemo B (2002) 'Missing mass' effect in biosensor's QCM application. Biosens Bioelectron 17:835–841
170. Duncan-Hewitt WC, Thompson M (1992) Four-layer theory for the acoustic shear wave sensor in liquids incorporating interfacial slip and liquid structure. Anal Chem 64:94-105
171. Mak C, Daly C, Krim J (1994) Atomic-scale friction measurements on silver and chemisorbed oxygen surfaces. Thin Solid Films 253:190–193
172. Rodahl M, Kasemo B (1996) On the measurement of thin liquid overlayers with the quartz-crystal microbalance. Sens Actuators A 54:448–456
173. Hayward GL, Thompson M (1998) A transverse shear model of a piezoelectric chemical sensor. J Appl Phys 83:2194–2201
174. McHale G, Lucklum R, Newton MI, Cowen JA, Hauptmann P (2000) Influence of viscoelasticity and interfacial slip on acoustic wave sensors. J Appl Phys 88:7304–7312
175. Daikhin L, Gileadi E, Tsionsky V, Urbakh M, Zilberman G (2000) Slippage at adsorbate-electrolyte interface response of electrochemical quartz crystal microbalance to adsorption. Electrochim Acta 45:3615–3621
176. Ellis JS, McHale G, Hayward GL, Thompson M (2003) Contact angle-based predictive model for slip at the solid-liquid interface of a transverse-shear mode acoustic wave device. J Appl Phys 94:6201–6207

177. Ponomarev IV, Meyerovich AE (2003) Surface roughness and effective stick-slip motion. Phys Rev E 67:026302, 1–12
178. Theissen LA, Martin SJ, Hillman AR (2004) A model for the quartz crystal microbalance frequency response to wetting characteristics of corrugated surfaces. Anal Chem 76:796–804
179. Du B, Goubaidoulline I, Johannsmann D (2004) Effects of laterally heterogeneous slip on the resonance properties of quartz crystals immersed in liquids. Langmuir 24:10617–10624
180. Knoll W, Frank CW, Heibel C, Naumann R, Offenhäusser A, Rühe J, Schmidt EK, Shen WW, Sinner A (2000) Functional tethered lipid bilayers. Rev Molecular Biotechnol 74b:137–158
181. Boulbitch A, Guttenberg Z, Sackmann E (2001) Kinetics of Membrane Adhesion Mediated by Ligand-Receptor Interaction Studied with Biomimetic System. Biophys J 81:2743–2751
182. Cheng J-X, Pautot S, Weitz DA, Xie XS (2003) Ordering of water molecules between phospholipids bilayers visualized by coherent anti-Stokes Raman scattering microscopy. Proc Natl Acad Sci U S A 100:9826–9830
183. Goennenwein S, Tanaka M, Hu B, Moroder L, Sackmann E (2003) Functional incorporation of integrins into solid supported membranes on ultrathin films of cellulose: impact on adhesion. Biophys J 85:646–655
184. Burgess I, Li M, Horswell SL, Szymanski G, Lipkowski J, Satija S, Majewski J (2005) Influence of the electric field on a bio-mimetic film supported on a gold electrode. Colloids Surf B 40:117–122
185. Martin SJ, Frye GF (1991) Polymer film characterization using quartz resonators. IEEE Ultrason Symp Proceedings 393–398
186. Katz A, Ward MD (1996) Probing solvent dynamics in concentrated polymer films with a high frequency shear mode quartz resonator. J Appl Phys 80:4152–4163
187. Lucklum R, Behling C, Cernosek RW, Martin SJ (1997) Determination of complex shear modulus with thickness shear mode resonators. J Phys D Appl Phys 30:346–356
188. Lucklum R, Behling C, Hauptmann P, Cernosek RW, Martin SJ (1998) Error analysis of material parameter determination with quartz-crystal resonators. Sens Actuators A 66:184–192
189. Behling C, Lucklum R, Hauptmann P (1999) Fast three-step method for shear moduli calculation from quartz crystal resonator measurements. IEEE Trans Ultrason Ferroelec Freq Contr 46:1431–1438
190. Johannsmann D (1999) Viscoelastic analysis of organic thin films on quartz resonators. Macromol Chem Phys 200:501–516
191. Lucklum R, Hauptmann P Thin film shear modulus determination with quartz crystal resonators: a review 2001 IEEE Int Freq Contr Symp Proceedings 408–418
192. Garrell RL, Chadwick JE (1994) Structure, reactivity and microrheology in self-assembled monolayers. Colloids Surf A 93:59–72
193. Bund A, Schwitzgebel G (1998) Viscoelastic Properties of Low-Viscosity Liquids Studied with Thickness-Shear Mode Resonators. Anal Chem 70:2584–2588
194. Berg S, Johannsmann D (2003) High speed microtribology with quartz crystal resonators. Phys Rev Lett 91:145505, 1–4
195. Abdelmaksoud M, Bender JW, Krim J (2004) Bridging the gap between macro- and nanotribology: a quartz crystal microbalance study of tricresylphosphate uptake on metal and oxide surfaces. Phys Rev Lett 92:176101 1–4
196. Cavic BA, Thompson M (2002) Interfacial nucleic acid chemistry studied by acoustic wave propagation. Anal Chim Acta 469:101–113
197. Bailey LE, Kambhampati D, Kanazawa KK, Knoll W, Frank CW (2002) Using surface plasmon resonance and the quartz crystal microbalance to monitor in situ the interfacial behavior of thin organic films. Langmuir 18:479–489
198. Schlatt-Masuth B, Hempel U, Lucklum R, Hauptmann P (2004) QCR response to attachment processes of particles IEEE Sensors. Proceedings 790–793
199. Ellis J, Thompson M (2005) Signals from the acoustic shear wave biosensor explained. 345. WE–Heraeus Seminar. Acoustic Wave Based Sensors: Fundamentals, Concepts, New Applications
200. Wolff O, Seydel E, Johannsmann D (1997) Viscoelastic properties of thin films studied with quartz crystal resonators. Faraday Disc 107:91–104
201. Johannsmann, D (2001) Derivation of the shear compliance of thin films on quartz resonators from comparison of the frequency shifts on different harmonics: a perturbation analysis. J Appl Phys 89:6356–6364
202. Yoshimoto M, Tokimura S, Shigenobu K, Kurosawa S, Naito M (2004) Properties of the overtone mode of the quartz crystal microbalance in a low-viscosity liquid. Anal Chim Acta 510:15–19
203. Hempel U, Schlatt-Masuth B, Lucklum R, Hauptmann P (2004) QCR response to formation process of nanoparticles Eurosensors XVIII Techn Digest 150–151 CD:A5_3, pp 1–4
204. Hillman AR, Jackson A, Martin SJ (2001) The problem of uniqueness of fit for viscoelastic films on thickness shear mode resonator surfaces. Anal Chem 73:540–549
205. Martin SJ, Frye GC, Ricco AJ, Senturia SD (1993) Effect of surface roughness on the response of thickness shear mode resonators in liquids. Anal Chem 65:2910–2922
206. Urbakh M, Daikhin L (1998) Surface morphology and the quartz crystal microbalance response in liquids. Colloids Surf A 134:75–84
207. Daikhin L, Gileadi E, Katz G, Tsionsky V, Urbakh M, Zagidulin D (2002) Influence of roughness on the admittance of the quartz crystal microbalance immersed in liquids. Anal Chem 74:554–561
208. Kuroiwa M, Nakazawa M (2002) An analysis of plate surface roughness effect for AT-cut resonators, IEEE Frequency Control Symposium Proceedings 242–247
209. EerNisse EP (1972) Simultaneous Thin-Film Stress and Mass-Change Measurements Using Quartz Resonators. J Appl Phys 43:1330–1337
210. Barthé PG, Benkeser PJ (1987) A staircase model of tapered piezoelectric transducers. IEEE Ultrason Symp Proceedings 697–700
211. Martin BA, Hager HE (1989) Velocity profile on quartz crystals oscillating in liquids. J Appl Phys 65:2630–2635
212. Tessier L, Patat F, Schmitt N, Feuillard G, Thompson M (1994) Effect of the generation of compressional waves on the response of the thickness-shear mode acoustic wave sensor in liquids. Anal Chem 66:3569–3574
213. Lin Z, Ward MD (1995) The role of longitudinal waves in quartz crystal microbalance applications. Anal Chem 67:685–693
214. Schneider TW, Martin SJ (1995) Influence of compressional wave generation on thickness-shear mode resonator response in a fluid. Anal Chem 67:3324–3335
215. Lucklum R, Schranz S, Behling C, Eichelbaum F, Hauptmann P (1997) Analysis of compressional-wave influence on thickness-shear-mode resonators in liquids. Sens Actuators A 60:40–48
216. Mc Kenna L, Newton MI, McHale G, Lucklum R, Schroeder J (2001) Compressional acoustic wave generation in microdroplets of water in contact with quartz crystal resonators. J Appl Phys 89:676–680
217. Lucklum R, Hauptmann P (2002) Generalized Acoustic Parameters of Non-Homogeneous Thin Films IEEE Int Freq Contr Symp Proceedings 234–241
218. Ricco AJ, Martin SJ, Zipperian TE (1985) Surface acoustic wave gas sensor based on film conductivity changes. Sensors Actuators 8:319–333

219. Shana ZA, Zong H, Josse F, Jeutter DC (1994) Analysis of electrical equivalent circuit of quartz crystal resonator loaded with viscous conductive liquids. J Electroanal Chem 379:21–33
220. Shana ZA, Josse F (1994) Quartz crystal resonators as sensors in liquids using the acoustoelectric effect. Anal Chem 66:1955–1964
221. Lee Y, Everhart D, Josse F (1996) The quartz crystal resonator as a detector of electrical loading: An analysis of sensing mechanism IEEE Int Freq Contr Symp Proceedings 577–585
222. Ghafouri S, Thompson M (2001) Electrode modification and the response of the acoustic shear wave device operating in liquids. Analyst 126:2159–2167
223. Zhang C, Vetelino J (2001) A bulk acoustic wave resonator for sensing liquid electrical property changes IEEE Int Freq Contr Symp Proceedings 535–541
224. Lee PCY (1989) Electromagnetic radiation from an AT-cut quartz plate under lateral-field excitation. J Appl Phys 65: 1395–1399
225. Hu Y, French LA Jr, Radecsky K, da Cunha MP, Millard P, Vetelino JF (2004) A lateral field excited liquid acoustic wave sensor. Trans Ultrason Ferroelectr Freq Contr 51:1373–1380
226. Hu Y, Pinkham W, French LA Jr, Frankel D, Vetelino JF (2005) Pesticide detection using a lateral field excited acoustic wave sensor. Sens Actuators B 108:910–916
227. Bjurström J, Katardjiev I, Yantchev V (2005) Lateral-field-excited thin-film Lamb wave resonator. Appl Phys Lett 86: 154103–154105
228. Laschitsch A, Menges B, Johannsmann D (2000) Simultaneous determination of optical and acoustic thicknesses of protein layers using surface plasmon resonance spectroscopy and quartz crystal microweighing. Appl Phys Lett 77:2252–2254
229. Kim J, Yamasaki R, Park J, Jung H, Lee H, Kawai T (2004) Highly dense protein layers confirmed by atomic force microscopy and quartz crystal microbalance. J Bioscience Bioeng 97:138–140
230. Smith AL, Shirazi HM (2005) Principles of quartz crystal microbalance/heat conduction calorimetry: measurement of the sorption enthalpy of hydrogen in palladium. Thermochim Acta 432:202–211
231. Shevade AV, Ryan MA, Homer ML, Kisor AK, Manatt KS, Lin B, Fleurial JP, Manfred AM, Yen SPS (2005) Calorimetric measurements of heat of sorption in polymer films: A molecular modeling and experimental study. Anal Chim Acta 543:242–248
232. Fadel L, Zimmermann C, Dufour I, Dejous C, Rebiere D, Pistre J (2005) Coupled determination of gravimetric and elastic effects on two resonant chemical sensors: love wave and microcantilever platforms. IEEE Trans Ultrason Ferroelectr Freq Contr 52:297–303
233. Su X, Wu YJ, Robelek R, Knoll W (2005) Surface plasmon resonance spectroscopy and quartz crystal microbalance study of MutS binding with single thymine-guanine mismatched DNA. Front Biosci 10:268–274
234. Su XX, Wu YJ, Robelek R, Knoll WW (2005) Surface plasmon resonance spectroscopy and quartz crystal microbalance study of streptavidin film structure effects on biotinylated DNA assembly and target DNA hybridization. Langmuir 21:348–353
235. Zhang H, Zhao R, Chen Z, Shangguan DH, Liu G (2005) QCM–FIA with PGMA coating for dynamic interaction study of heparin and antithrombin III. Biosens Bioelectron 21:121–127